Ctenolepis garcinii - Green Synthesized Silver Nanoparticles Induced Apoptotic Cell Death in MDA-MB-231 Breast Cancer Cells by Generating Reactive Oxygen Species and Activating Caspase 3 and 9 Enzyme Activities

Anuradha.R,

PG and Research Department of Biochemistry,SengamalaThayaar Educational Trust Women's College (Autonomous),Sundarakkottai, Mannargudi, Thiruvarur DT, Tamilnadu, India.

ABSTRACT

One of the most important diagnostic and therapeutic tools in the field of nanomedicine is the silver nanoparticle. The significant anticancer herb *Ctenolepis garcinii* ethanolic extract was used in the current study to optimize a cost-effective production technique for silver nanoparticles. We looked at AgNPs ability to fight cancer and their probable role in apoptosis. The crystal sizes of the stable, spherical, biosynthesized AgNPs range from 20 to 51 nm. Breast cancer MDA-MB-231 cells exhibit concentration-dependent growth suppression in the MTT cell viability assay (IC50, 9.5 µg/mL). Additionally, the fluorescence microscopic analysis demonstrates that AgNPs activate caspases 3 and 9, which result in nuclear condensation (DAPI assay) and morphological alterations (AO/EB assay) in the cell membrane, both of which ultimately result in apoptotic cell death (Annexin V/PI test). Additionally, it was shown that AgNPs cause MDA-MB-231 cells to produce reactive oxygen species (ROS) and mitochondrial membrane potential, which regulate oxidative stress. This is the first study to describe the creation of a silver nanoparticle by the action of a *Ctenolepis garcinii* extract and an analysis of the cellular and molecular mechanisms underlying apoptosis.

Key Words: *Ctenolepis garcinii*, MTT, ROS, caspases 3 and 9.

Introduction

The leading factor in deaths among women worldwide is breast cancer. For its therapy, a variety of chemotherapeutic methods can be used. They do come with scary side effects, though, and are expensive. In addition, the various current chemotherapies are losing their effectiveness on breast cancer cells [1]. Finding alternative therapy options that are effective, affordable, and biocompatible is therefore imperative. Due to their numerous applications, metal and metal oxide nanoparticles have recently emerged as an exciting topic of research [2–8]. In the biomedical sciences, where it supports therapies and diagnostics,

nanobiotechnology has notable uses [9–11]. AgNPs have recently been the subject of extensive research due to their intriguing physical, biological, and medicinal features [12, 13].

The synthesis of AgNPs uses a variety of chemical and physical techniques [14]. These techniques have various drawbacks despite being efficient. The chemical and physical processes need a lot of energy resources and produce hazardous waste and harmful byproducts [5, 15]. According to recent studies, chemically produced nanoparticles are largely unsuitable for biomedical uses since they contain toxic compounds [16]. AgNPs are synthesized using entirely green processes to avoid harmful byproducts and the problem of energy balance. As a result, a paradigm change in favour of AgNPs' biological production is seen. To create nanoparticles, a variety of biological resources, including plants, bacteria, algae, and yeasts, are utilised [17]. However, plants and plant products are the most often utilized method for the production of nanoparticles due to their wide availability, low cost, and rich source of bioreducing agent [18, 19]. The advantages of biosynthesis over other processes are its quickness, low cost, single-step synthesis, high yield, and biocompatibility [20]. Additionally, the size can be readily altered by modifying the pH, temperature, and salt concentrations.

A fascinating area of research for those looking for less expensive and alternative chemotherapeutics is the intersection of medicinal plants, nanoparticles, and cancer. In this study, we refined an entire green process for the phytosynthesis of AgNPs using an ethanolic extract of the crucial *Ctenolepis garcinii* plant. Indigenous knowledge suggests that *Ctenolepis garcinii* may have anticancer effects. The Tamils employ this species as a remedy for quinsy and other throat conditions [21]. Recent studies further revealed that *Ctenolepis* has powerful anticancer properties against HepG-2 cells [22]. There have been reports of the biological production of AgNPs so far [13, 23, 24]; however, to date, no reports are available to study the anticancer mechanism of the phytosynthesized AgNPs mediated by the ethanolic extract of *Ctenolepis garcinii*. This groundbreaking work explores the cellular and molecular pathways of apoptosis brought on by AgNPs produced by *Ctenolepis* extract. Previous research demonstrates the biological characteristics of biogenic AgNPs, such as antimicrobial [25–29], anticancerous [30–32], antiangiogenic, antiparasitic [33,34], cytotoxic [35–38], and antitumor [39, 40]. varied AgNPs have varied impacts on the destruction of cancer cells. By disrupting the membrane integrity and regular cellular processes, Sanpui and his coworkers showed that AgNPs caused apoptosis [41]. Human cervical cells treated with AgNPs underwent apoptosis, according to Vasanth and his colleagues [30].

The most popular forms of treatment for breast cancer are still chemotherapy and combination chemotherapy [42]. However, because of their potential drawbacks, it is essential to hunt for complementary and potent medical procedures. With the help of medicinal flora, the goal of the current

study was to create silver nanoparticles utilizing a quick, safe technique. In addition, MDA-MB-231 breast cancer cells were used to test the phytosynthesized AgNPs for their anticancer activity while several mechanistic assays were used to elucidate the anticancer compounds' mechanism.

Material and methods

All of the chemicals were of the analytical grade and were utilized directly out of the container without further purification. With deionized water, all solutions were made.

Preparation of extract

Fresh *Ctenolepis garcinii* leaves were properly cleansed with distilled water after being thoroughly washed with tap water. The leaves were allowed to dry at room temperature for a week before using a Starlite blender (Model SL-999) to grind them into a fine powder. Weighting out (20 gm) of the milled powdered *Ctenolepis garcinii* was steeped in 300 ml of ethanol in a conical flask, and vigorous stirring with a glass rod was used to ensure efficient extraction. At room temperature, the mixture was given 24 hours to settle. After being filtered using Whatman no. 1 filter paper (125 mm 100 circles), the extracts were then employed in additional tests.

Synthesis of silver nanoparticles

Silver nanoparticles (AgNPs) were created by reacting an ethanol extract of *Ctenolepis garcinii* leaves with 300 c of AgNO3 (2 mM) in an Erlenmeyer flask. This setup was incubated at 37 °C under static conditions in the dark (to reduce the photoactivation of silver nitrate). A control setup without any *Ctenolepis garcinii* leaf extract was also kept. The tint transitions from light yellow to dark brown.

Characterization of AgNPs

The synthesized AgNPs were first verified and characterized using a UV-vis spectrophotometer (Shimadzu UV-1800 UV/Visible Scanning Spectrophotometer; 115 VAC) operating with a 1 nm resolution in the absorbance range of 200–700 nm [43]. Periodic sampling was used to track the bioreduction of the Ag+ ions (AgNO3) in solution by the ethanol plant extract. By employing XRD analysis (Shimadzu XRD-6000/6100 model) and Cu-K radiation with the scattering 2 range of 20–80, the phase nature, and lattice parameters of the green produced AgNPs were found. The instrument was operated at 30kv with a current of 30º mA [44]. FTIR analysis was used to examine the functional groups of the AgNPs made from aqueous leaf extract (Perkin Elmer, USA). The KBr disc was coated with the powder form of the air dried nanoparticles, which were then analyzed at a resolution of 4 cm1, ranging from 400 to 4000 cm 1 [45]. SEM (ZEISS) analysis of the morphological characteristics of green Silver Nanoparticles produced

synthetically. The material was formed into thin films and placed on a copper grid that had been coated with carbon for this electron microscopic investigation. Images were then captured. The purity, size, and morphology of the *C.garcinii* AgNPs mediated by the aqueous leaf extract were examined using TEM (JEM-Z300FSC (CRYO ARMTM 300)). The sonicated and dried AgNPs were coated on copper grids with carbon before being vacuum dried overnight and examined under TEM [46].

Cell Culture

Breast cancer MDA-MB-231 cells were cultured in Dulbecco's modified Eagle's medium (DMEM), pH = 7:2, with 10% FBS added. To avoid any cross contamination, Penicillin (100 U/ml) was also added to the media. Cells were incubated in a humidified incubator with 5% CO2. Trypsin was employed to collect the cell population (80–90%), which was then washed in PBS and used in subsequent studies.

Cell Viability Assays

To test the vitality of cells, the previously described MTT cytotoxicity evaluation technique was employed with a few minor modifications [47]. After being cultivated to a density of 1 × 104 cells/well for 24 hours, cancer cells were exposed for 24 hours to various test AgNP concentrations. Following that, 10 L of PBS with added 5.0 mg/mL MTT were added to each well and incubated for an additional 4 hours. As a result of the addition of MTT, formazan crystals began to grow inside the living cells. The formazan crystals were dissolved with DMSO (100 L).

Inhibitory of cell proliferation (%) = Mean absorbence of the control − Mean absorbence of the sample/ Mean absorbence of the control X 100

Morphological Study with Fluorescence Microscopy

AO/EB fluorescence staining techniques were used to examine AgNP-treated MDA-MB-231 cells to determine the level of apoptosis [48]. Briefly, MDA-MB-231 cells were cultured in six-well plates for 24 hours at a density of 5 x 104 cells per well. After that, cells were subjected to the inhibitory concentration (IC500) for 24 hours. Cells that weren't exposed to AgNPs were used as the control. The two dyes, which had previously been produced at 100 g/mL in PBS each, were combined to create a mixture of the AO/EB dyes (20 L). These cells were observed and imaged using an Olympus fluorescence microscope with excitation (488 nm) and emission (520 nm) after staining the treated and control samples.

Observation of Chromatin Changes

To further investigate the chromatin changes that are a crucial component of the apoptosis process, the 4,6-Diamidino-2-phenylindole (DAPI) staining experiment was used [49]. In cells that have experienced the process of apoptosis, the fluorescent dye DAPI was created for staining nuclear DNA. In a nutshell, cells (MDA-MB-231) were cultured to a density of 2 105 cells per well and added to 24-well plates during the log phase, followed by 24 hours of incubation. The culture was then maintained for up to 24 hours after the application of the IC50 concentrations of green synthesized AgNPs. After the procedure, 50 L of a 1:1 mixture of water and methanol was used to fix the cells before washing them with 1x PBS. For staining, 100 L of DAPI dye diluted to 1 g/mL were employed, followed by a 30-minute dark incubation period at 37 °C. For the purpose of removing the extra colour, 20 L of PBS: glycerin (1:1) was added. Under a 40x inverted fluorescent microscope, chromatin changes were seen. Apoptotic cells were expressed in percentage calculated as

$$\% \text{ apoptotic cells} = (\text{amount of apoptotic nuclei amount of all cells}) \times 100$$

Cell Apoptosis Assay

PI staining was utilized to quantify the degree of apoptosis. The MDA-MB-231 cells were added to the 24-well plate with DMEM at a density of 1106 cells per well and incubated for 24 hours at 37°C. The MDA-MB231 cells were then re-incubated for 24 hours at 37°C with the addition of 9.5 g of AgNPs. Following the incubation, the PI stain [50] was added to each well, and the plate was then left in a dark area for 20 minutes to stain the cells. Using a fluorescent microscope, apoptotic cell death was finally examined.

Cell adhesion assay

By repeatedly ingesting trypsin, cells were harvested. Cells were next added to 96-well plates. In order to remove cells that had become anxiously attached, wells containing the separated cells were washed with PBS and medium at intervals of 0, 15, 30, 45, and 60 minutes. Paraformaldehyde (5%) was used to develop the cells beneath the plate, and trypan blue dye (1%) was then added, and the cells were fostered for 15 minutes. Extra trypan blue dye was washed up by PBS 48 after 15 minutes of staining. The cellular proteins were attached to trypan blue. The amount of trypan blue that was converted to protein was related to the number of cells in the well. Trypan blue was removed after being exposed to air by familiarizing isopropanol, and the absorption of blue colour was reflected at 540 nm in a microplate reader [51].

Mitochandrial Membrane Potential

The selectivity for mitochondria and the fluorescent features of the laser dye Rh-123 are used to demonstrate that it is a selective probe for the localization of mitochondria in living cells. MDA-MB-231 cells were put into a six-well plate with a cover slip and treated with 9.5 g/ml of AgNps at various concentrations. Rh-123 dye was used to stain the cells, and the incubation time was 15 minutes. Cells were fixed after two PBS washes. At a wavelength of 535 nm, the fluorescence intensity was measured, and the proportion of MDA-MB-231 cells that showed pathological alterations was determined.

Quantification of Caspase 3 and 9 Activities

Caspase activity were measured using caspase 3 and 9 assay kits (Caspase-Glo® 3 and 9 reagents, Promega). In a 96-well plate, 50,000 MDA-MB-231 cells were seeded each well. The cells underwent a 24-hour incubation period in a humidified incubator with 5% CO2 at 37° C. The 96-well plates with control cells that had not been exposed to AgNPs and those that had were then allowed to acclimatize at room temperature. A 96-well plate with 100 L of culture media in each well (test well and control well) was filled with 100 L of Caspase-Glo® 3 or 9 reagent. The plate was covered, and the mixture was spun at 500 rpm for 30 seconds. After the plate had been incubated at room temperature for 30 minutes, the optical density was assessed (using an ELISA reader from BioTek) at 405 nm.

ROS Assay in MCF-7 Cells

The generation of intracellular ROS was examined using dichlorofluorescein diacetate (DCFDA) probes [52]. Briefly, MCF-7 cells were plated in 12-well plates for 24 h, after which they were exposed to AgNPs at the IC50 concentration for 24 h. The cells were separated with trypsin EDTA. PBS was used to clean the cells, then 200 mL of PBS with a 10 mM DCFH-DA fluorescent probe was used to resuspend the cells. At 37 degrees Celsius, the reaction mixture was incubated for 30 minutes. A fluorescence spectrophotometer was used to measure the amount of ROS produced [53].

Data Analysis

Cytotoxicity of the nanoparticles was expressed as the concentration (µg/mL) inhibiting the growth of 50% cells (IC50). Data was analyzed through MS Excel 2017, and IC50 was estimated through TableCurve 2D software. The graphs were prepared with OriginPro 8.1 and GraphPad.

Results and Discussions

Biosynthesis

The extract of *Ctenolepis garcinii* has been used to optimize the green biosynthesis of AgNPs. Comparing biological synthesis to physical and chemical techniques, it is thought to be the most effective technique. Although effective, up to this point, these physical and chemical synthesis methods have some drawbacks, such as high costs, energy requirements, and the production of toxic hazardous waste streams. [15,54]. Additionally, several research indicated that some harmful substances might stay attached to nanoparticles made by chemical techniques but not suitable for biological uses [16,55]. As a result, biomodulated AgNP production is chosen. The therapeutic potential of Ctenolepis garcinii, a significant medicinal herb, is widely known. According to recent findings, Ctenolepis garcinii has a significant anticancer potential when used in vitro [56]. The unique saponins, flavonoids, phenols, and triterpene chemical components of Ctenolepis are thought to be responsible for its therapeutic potential. These phytochemicals chelate and stabilize the nanoparticles throughout their production. Although the biogenic synthesis of Ag nanoparticles using plants has been successfully documented, it is uncommon for biosynthesis to use pharmaceuticals with anticancer potential. In Figure 1, a potential biosynthetic mechanism is presented.

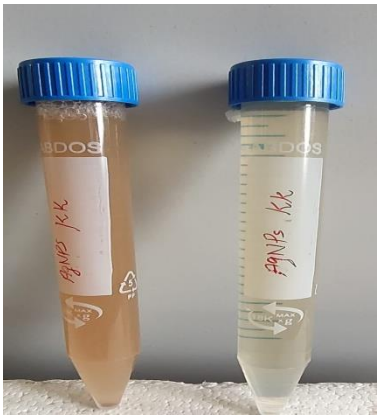

Figure 1: Variation in color intensity of green silver nanoparticles mediated at AgNO3 by leaf extracts

UV-Vis Spectrophotometry

UV-vis spectroscopy in the 100–800 nm region was used to further establish the green colour of the produced AgNPs. The presence of the green produced AgNPs was confirmed by a strong and distinct Surface Plasmon Resonance (SPR) signal at 280 nm (Fig. 2). The acquired peak value was nearly identical

to the earlier findings that showed the SPR peak at 280 nm and verified the AgNPs made from Capsicum annuum L. plant extract. **[57]**. The peak at 280, 340, and 360 nm indicated that the AgNPs were made from the Acacia ehrenbergiana plant [58]. UV-vis absorption peaks in Ag-NPs and the *Ctenolepis garcinii* extract both point to the capping function of phytochemicals in preventing Ag-NP aggregation.

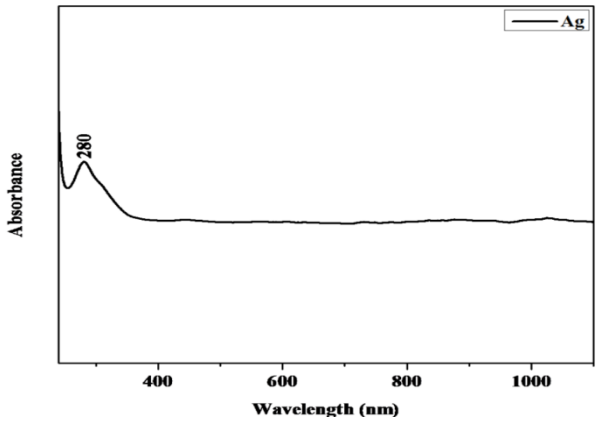

Figure 2: Optimization of different parameters for bioinspired synthesis of silver nanoparticles. UV-vis spectrum of AgNPs mediated by leaf ethanol extracts of *Ctenolepis garcinii*

X-Ray Diffraction (XRD)

Silver nanoparticle crystallinity was evaluated by XRD analysis. The XRD pattern of AgNPs produced during biosynthesis is shown in Figure 3. The observed Bragg peaks were discovered to be consistent with crystallographic reflections from the Cg-AgNPs diffraction planes 111(32.02°), 200(45.98°), 220(64.28°), and 311(77.22°), in that order. The other peaks, however, may have been caused by organic phytochemicals in the plant extract that serve as capping agents or by silver oxide crystal diffraction planes that may be covered on the surface of the Cg-AgNPs. Because of this, the existence of the (111) diffraction planes with the highest peak intensity proves that the Cg-AgNPs formed [59, 60, 61, 62]. However, the existence of the additional diffraction planes offers more proof in favour of the phytochemicals function as capping agents, which is compatible with the FTIR and UV-vis spectrum analyses [63, 64].

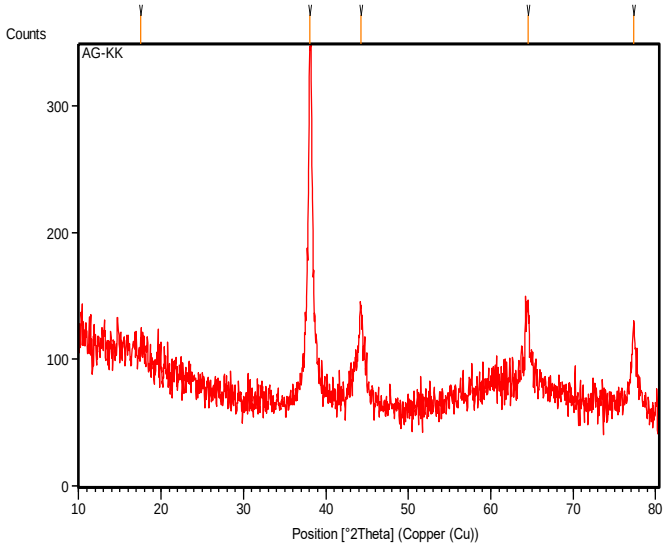

Figure 3: X-ray diffraction (XRD) pattern of green-synthesized AgNPs showing Bragg reflection at angle 2 theta

FTIR spectra

Figure 4 shows the FTIR spectra of AgNPs powders produced using the precursor. Various absorption peaks were found in the 4000–400 cm-1 range. The primary amine bond's N-H stretching is indicated by the large absorption peak at 3450 cm-1. The strength of the peak associated with the C-N of the aromatic amine bond was diminishing when the precursor concentrations were reduced. The isocyanate compounds N-C=O stretching is shown by the peaks that can be seen from 2073 to 1044 cm-1.

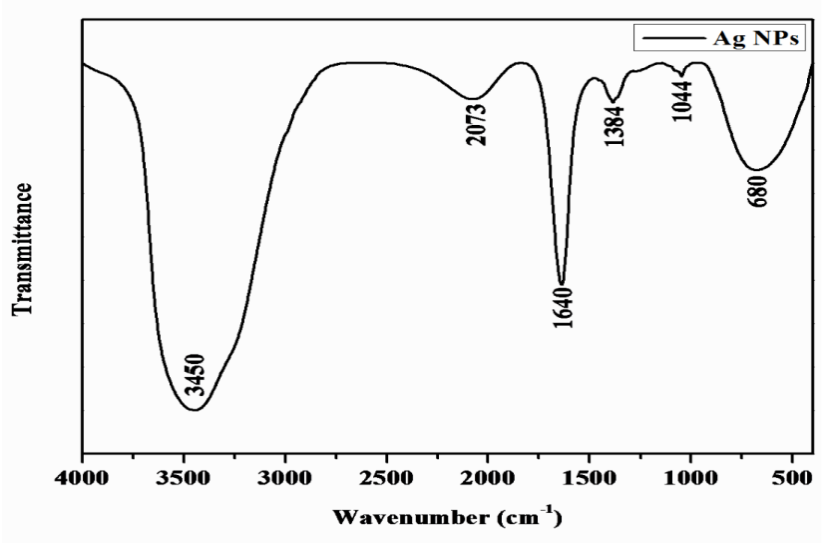

Figure 4: FTIR spectra of extract Cg−AgNPs show different absorption peaks pertaining to the existence of extract biomolecules on the surfaces of nanoparticles.

Scanning Electron Microscopy (SEM)

In Figure 5, a SEM micrograph is shown. The polydispersed nanoparticles with low agglomeration are shown in the figure. The nanoparticles' spherical (20–50 at 200 nm scale) form was noticed. Using an extract from the Cassia fistula flower, Remya *et al.* produced nanoscale silver with a size range of 25–51 nm [65]. Results from AgNPs synthesized using *Acalypha indica* and *Syzygium alternifolium* were similar [24, 66].

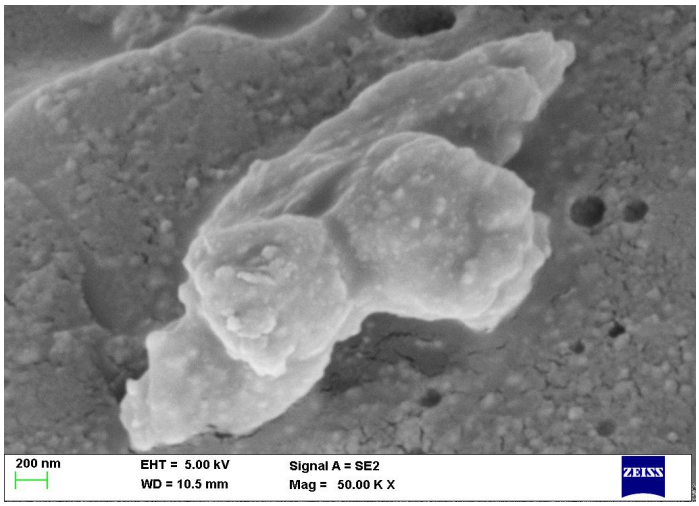

Figure 5: Morphology of Cg-AgNPs SEM micrograph at the scale of 200 nm shows spherical nanoparticles.

TEM

Through TEM investigation, the AgNPs synthesized from the *C. garcini* extract are precisely depicted in **Fig. 6** in terms of their morphology. From plant extract, spherical Cg-AgNPs in the 25–50 mm range has been produced. This shape homogeneity has been linked to the SPR peak discovered during the UV-vis investigation. Similar to this, it has been reported that *Tectona grandis* extract was used to create AgNPs that were 10–30 nm in size and spherical in form [67]. The reduction of AgNO3 into particles with a size between 10 and 25 nm may be caused by the phytochemicals that are the most active [28]. *Ocimum gratissimum* and *Ocimum sanctum* were used to create AgNPs [68]. The AgNPs synthesized using *Ocimum sanctum*, and *Ocimum gratissimum* [69], *Senna siamea, Crossopteryx febrifuga, and Brillantaisia patula* also had comparable peak types that corresponded to the functional groups involved in bioreduction [70].

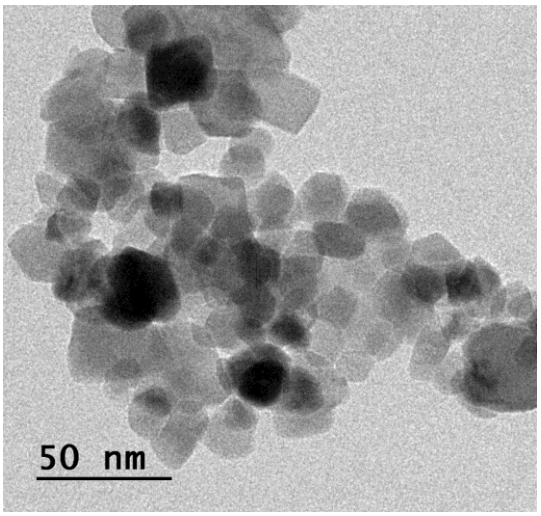

Figure 6: TEM image reveals the morphology of individual nanoparticles.

Cytotoxicity. 3-(4,5-Dimethylthiazol-2-Yl)-2,5-diphenyltetrazolium bromide

To assess the cytotoxicity of the extract and Cg-AgNPs in MDA-MB-231 cells, a cell viability experiment was performed. The MDA-MB-231 cells % growth inhibition was compared to that of untreated cells at various dosages (2.5–15 µg/ml). In vitro grown breast cancer cells exhibit a concentration-dependent growth inhibition in Figure 7. The IC50 value for cells treated with Cg-AgNP was determined to be 9.5 µg/ml. In this work, additional trials were conducted using this 50% lethal concentration. Similar findings from earlier studies looking at the impact of green-synthesized AgNPs in MCF-7 cells are shown here. [22, 71, 72].

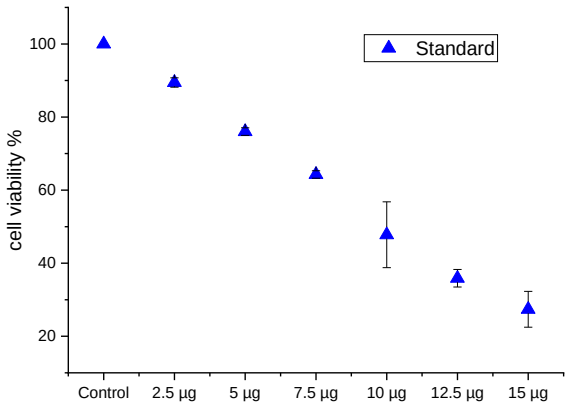

Figure 7: Cytotoxicity of extract Cg-AgNPs in MDA-MB-231 cells.

Acridine Orange-Ethidium Bromide (AO/EB) Fluorescent Assay

The morphological alterations in MDA-MB-231 cells were examined using the AO/EB fluorescent microscopic staining method. Differentiating between apoptotic and healthy cells uses AO/EB labelling. Figure 8 displays the 9.5 µg/ml (Cg-AgNPs) concentrations of the control untreated, extract, and Cg-AgNP-treated cells after 24 hours. The illustration demonstrates that whereas treated cells changed colour from green to orange, signifying apoptotic cells, control cells did not change and remained green after labelling. The treated cells additionally exhibit membrane blebbing, shrinkage, and nuclear disintegration. Similar membrane alterations were seen in breast cancer cells treated with Morinda pubescens-produced silver nanoparticles [73], *Teucrium stocksianum* extract-mediated AgNPs [24], *Syzygium aromaticum* extract-mediated AgNPs [22, 74], and *Solanum trilobatum* fruit extract silver nanoparticles [75].

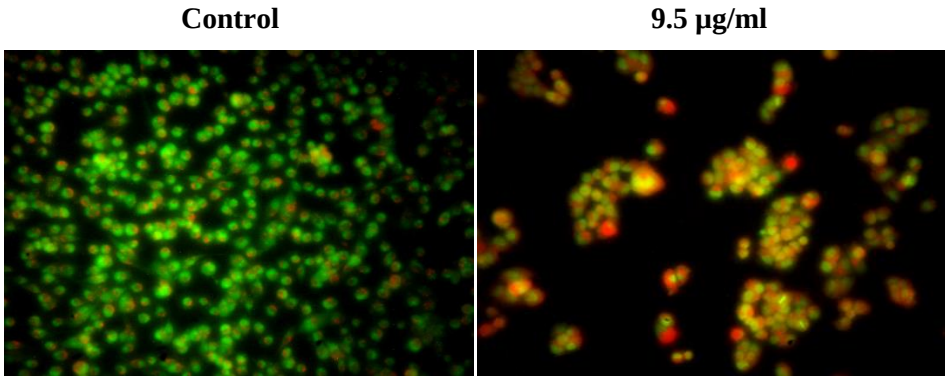

Figure 8: Morphological observation of MDA-MB-231 cells treated with extract Cg-AgNPs.

Nuclear Morphology

Using the DAPI staining technique, the effect of AgNPs on nuclear alterations was seen. After Cg-AgNP treatment for 24 hours, DAPI staining of the treated cells shows a substantial difference in the shape of the chromatin nuclear material compared to the untreated control, as shown in Figure 9. The treated cells had a brilliant colour, aberrant nuclei, condensed chromatin, and uneven cell structure, in contrast to the control cells normal, rounded nuclei and blue colour. These findings support those of Ciftci *et al.*, [76]. Our findings are consistent with earlier research on the impact of plant alkaloids and green-synthesized AgNPs on apoptosis in breast cancer cells [22, 77, 78]. Fluorescence microscopy was used to confirm the apoptosis in more detail.

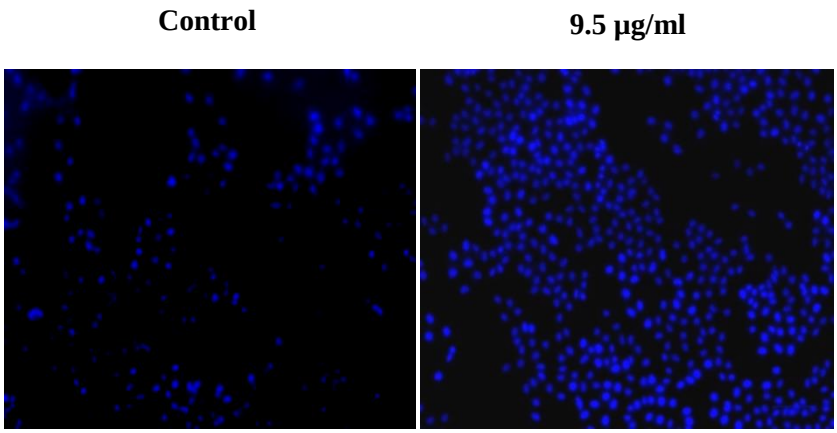

Figure 9: The changes were observed with DAPI nuclear staining of the treated cells.

Cell adhesion assay

After a 24-hour treatment, *C.garcini* was able to reduce the MDA-MB-231 cell's adhesion capacity (Figure 9). Which may aid to prevent cancer cells from separating from the primary tumour and preserve the adhesion stability of the primary cancer cells.

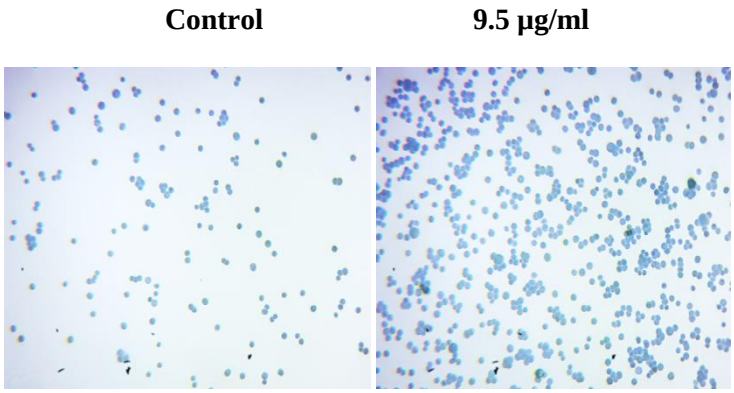

Figure 9: The cell adhesion were observed.

Mitochondrial membrane potential

The variation in the mitochondrial membrane potential level is shown by MMP labelling. MMP level is significantly induced in MDA-MB-231 cells treated with produced silver nanoparticles compared to control. Figure 10 This finding indicated that nanoparticle-induced cell death is caused by the integrity of the mitochondrial membrane. It is also widely known that high levels of ROS production can cause

cellular damage by damaging the mitochondrial membrane, which can ultimately cause toxicity [79,80]. Based on cationic fluorescent probe Rh123 dye, the increase in MMP level suggested that oxidative stress and the production of reactive oxygen species had a role in the death of MDA-MB-231 cells caused by free radicals induction by silver nanoparticles [81].

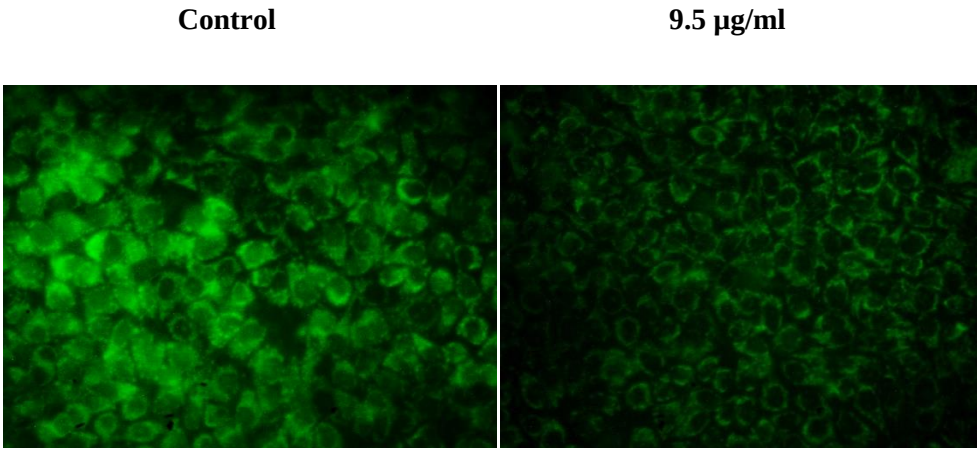

Figure 10: The Cell mitochondrial membrane potential level were observed

Annexin V/Propidium Iodide Apoptosis Detection Assay

The assay for Annexin V/PI staining was performed to further confirm apoptosis. The test showed that cancer cells exposed to AgNPs (9.5 µg/mL) for 24 hours underwent apoptosis. Figure 11 demonstrates that cells left untreated did not exhibit any discernible apoptosis. After 24 hours, cells treated with Cg-AgNPs go through an early apoptotic cell population of 43.05% and an early apoptotic cell population of 23.62%. The number of viable cells has changed, which suggests that the anticancer effects of Cg-AgNPs have caused the cell to undergo apoptosis. Similar to this, Sriram and colleagues investigated AgNPs' anticancer effects in a tumour model and noticed a reduction in the tumour volume. [39]. Furthermore, the increased anticancer activities in MCF-7 cells are caused by a variety of metabolic pathways that silver nanoparticles activate Liang *et al* [82] and Venugopal *et al.* [68] observed that green-synthesised silver nanoparticles coupled with hyaluronic acid caused lipid peroxidation, autophagy, mitochondrial malfunction, and death in cells.

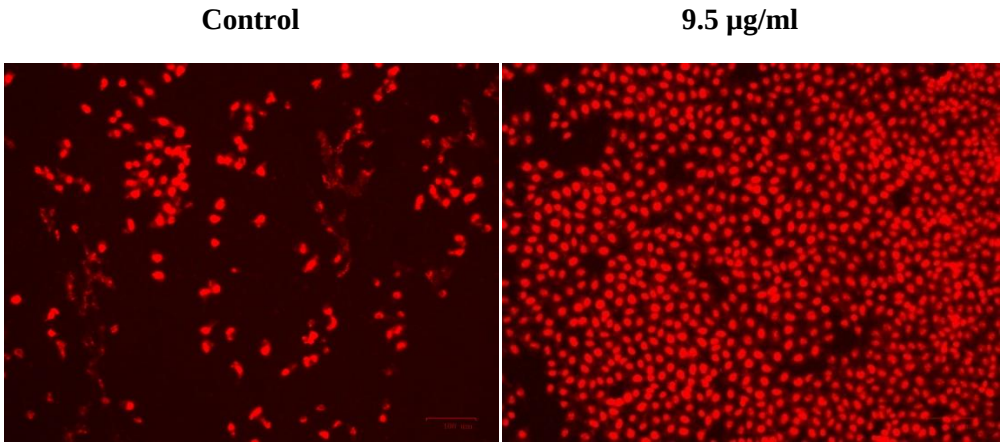

Figure 11: The analysis of MDA-MB-231 cells by double-labelling with Annexin V and PI dyes. The figure shows the early apoptotic, late apoptotic, live, and dead cells given in each quadrant of the untreated growth control cell compared to Cg-AgNP treated cells.

Caspase 3 and 9 Activities

The process of controlled cell death known as apoptosis manifests as the disassembly of intracellular components without causing injury or inflammation to neighbouring cells [83]. Caspases play a role in controlling inflammatory reactions and cell death [84]. In terms of functionality, there are two primary types of caspases: effector caspases (caspases 3, 6, and 7) and initiator caspases (caspases 2, 8, 9, and 10) [85, 86]. Caspase 3's interaction with caspases 8 and 9 causes apoptosis to begin. The apoptotic pathway similarly shows no return in this signal interaction [87]. By comparing the level of caspase 3 and 9 production in MDA-MB-231 cells treated with Cg-AgNP extract to the untreated control group, the apoptosis was further confirmed. When triggered by environmental factors, caspases 3 and 9 are the major cell death inducers in the terminal phase of cancer cells. When compared to untreated (control) cells, the activities of caspase 3 and 9 were two times higher in cells exposed to Cg-AgNPs extract. The outcomes agree with those of Kikuchi *et al* [88, 89]. The nucleus and membrane morphological changes raise the possibility that silver nanoparticles have a role in causing cancer cells to undergo apoptosis [22]. A number of initiator caspases, such as caspase 9, and executioner caspases, such as caspase 3, are expressed during apoptosis as an inactive zymogen that aids in the program of cell death [90, 91]. As depicted in Figure 12, AgNPs activate these caspases 3 and 9 as well as several other reactive oxygen species, which result in DNA damage, endoplasmic reticulum stress, protein misfolding, and death. According to reports, upon activation, caspase 3 fragments DNA by cleaving and translocating caspase-activated DNAse (CAD).

Endonuclease activity is thought to be a significant event in the early stages of apoptosis, which causes DNA frgmentation [92]. Arora *et al.* who were investigating the impact of AgNPs on cellular responses made a similar observation [93].

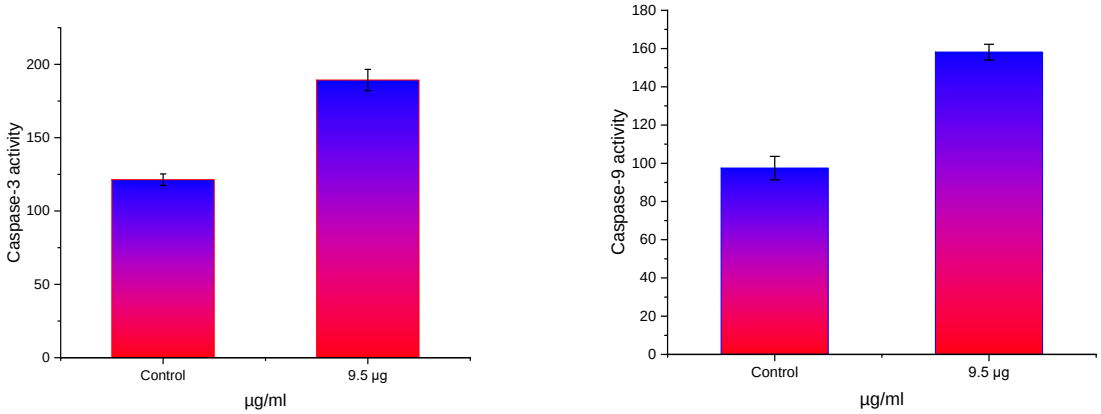

Figure 12: Quantification of caspase 3 and caspase 9 activity in MDA-MB-231 cells exposed to 9.5 µg/mL

Measurement of ROS (Reactive Oxygen Species)

The leading cause of apoptosis in cancer cells is the oxidative pressure created by the free radical produced in response to the environmental stimuli. According to earlier studies, Cg-AgNPs stimulate lipid peroxidation, which leads to death in cells, diminish mitochondrial potential, create oxidative stress, and restrict the activity of tumour suppressor genes [94]. Figure 13 depicts a potential process through which AgNPs may express apoptosis. Following the treatment of MDA-MB-231 cells with AgNPs (9.5 µg/mL), the ROS generation was assessed. A different time interval was used to compare the estimated ROS equivalent to H_2O_2 (M) to the untreated control cell. In comparison to control cells, Figure 13 shows the quantification of ROS in cells treated to Cg-AgNPs extract. Cg-AgNPs, as opposed to cells treated with extract, were more effective at producing ROS. The ability of the plant extract to scavenge certain free radicals may be the cause of this. After 16 hours, ROS production reached its peak and began to progressively decline. The concentrations and length of the therapy determine how ROS affect cellular events. Apoptosis, mitochondrial malfunction, and cell cycle arrest at the G0 phase are common biological reactions to stress [95]. It is suggested that the level of ROS-triggering chemicals be employed as a therapeutic agent that can kill cancer cells in a targeted manner [69, 96]. We found that the amount of ROS produced by AgNPs varies with time. AgNPs produce reactive oxygen species (ROS) in the NIH3T3 cell and cause mitochondria-dependent apoptosis via activating the JNP pathway, according to a study by Hsin

and colleagues [97]. Free radicals known as ROS are produced by the biological system as a result of regular cell function. The abnormal quantity of ROS causes cellular components to fail, resulting in DNA damage, lipid peroxidation, cell cycle arrest, caspase activation, and apoptosis [98].

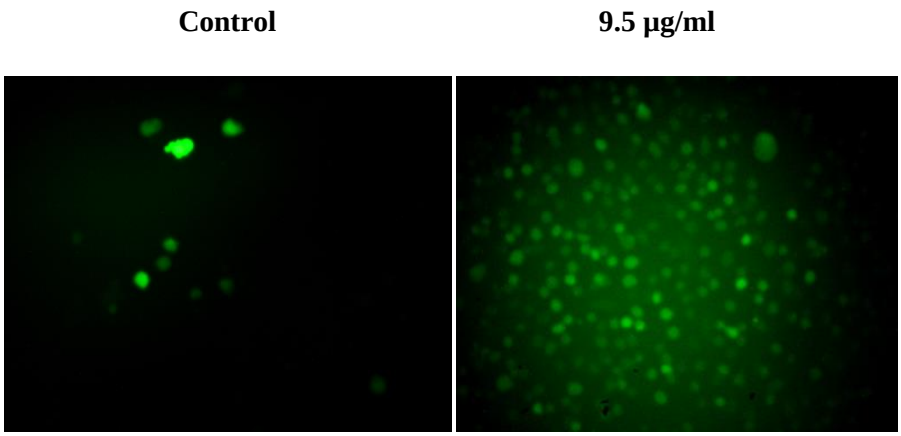

Figure 13: Effects of extract and AgNP exposition on ROS generation in MDA-MB-231 cells.

Conclusion

In this research, we describe a one-step biosynthesis of stable and environmentally friendly AgNPs using *C. garcinii* leaf extract under ideal conditions of 1 mM AgNO3. Additionally, regulated size nanoparticles (20–50 nm) were produced, and XRD, FTIR, SEM, and TEM investigations supported this finding. The antitumor activity elicited by the *C.garcinii* extract and AgNPs was concentration-dependent. By activating caspases, the NPs and extract cause membrane permeability, nuclear condensation in an apoptotic manner, and the production of reactive oxygen species. These nanoparticles may also be used in the creation of future anticancer medications.

ACKNOWLEDGMENT

Authoris thankful to the Management of Sengamala Thayaar Educational Trust Women's College (Autonomous), Mannargudi for providing financial support as seed money scheme and also provides all the necessary facilities related to the present research work.

Reference

1) V. Özmen, "Breast cancer in the world and Turkey," Journal of Breast Health, vol. 4, pp. 7–12, 2008

2) A. T. Khalil, M. Ovais, I. Ullah et al., "Sageretia thea (Osbeck.) mediated synthesis of zinc oxide nanoparticles and its biological applications," Nanomedicine, vol. 12, no. 15, pp. 1767– 1789, 2017.
3) A. T. Khalil, M. Ovais, I. Ullah et al., "Sageretia thea (Osbeck.) modulated biosynthesis of NiO nanoparticles and their in vitro pharmacognostic, antioxidant and cytotoxic potential," Artificial Cells, Nanomedicine, and Biotechnology, vol. 46, no. 4, pp. 838–852, 2018.
4) A. T. Khalil, M. Ovais, I. Ullah, M. Ali, Z. K. Shinwari, and M. Maaza, "Biosynthesis of iron oxide (Fe2O3) nanoparticles via aqueous extracts ofSageretia thea(Osbeck.) and their pharmacognostic properties," Green Chemistry Letters and Reviews, vol. 10, no. 4, pp. 186–201, 2017.
5) F. T. Thema, E. Manikandan, M. S. Dhlamini, and M. Maaza, "Green synthesis of ZnO nanoparticles via Agathosma betulina natural extract," Materials Letters, vol. 161, pp. 124–127, 2015.
6) F. T. Thema, E. Manikandan, A. Gurib-Fakim, and M. Maaza, "Single phase Bunsenite NiO nanoparticles green synthesis by Agathosma betulina natural extract," Journal of Alloys and Compounds, vol. 657, pp. 655–661, 2016.
7) S. Vasantharaj, N. Sripriya, M. Shanmugavel, E. Manikandan, A. Gnanamani, and P. Senthilkumar, "Surface active gold nanoparticles biosynthesis by new approach for bionanocatalytic activity," Journal of Photochemistry and Photobiology B: Biology, vol. 179, pp. 119–125, 2018.
8) M. Anbuvannan, M. Ramesh, E. Manikandan, and R. Srinivasan, "Vitex negundo leaf extract mediated synthesis of ZnO nanoplates and its antibacterial and photocatalytic activities," Asian Journal of Nanoscience and Materials, vol. 2, pp. 99–110, 2019.
9) S. Mukherjee, D. Chowdhury, R. Kotcherlakota et al., "Potential theranostics application of bio-synthesized silver nanoparticles (4-in-1 system)," Theranostics, vol. 4, no. 3, pp. 316–335, 2014.
10) S. Mukherjee, V. B, S. Prashanthi, P. R. Bangal, B. Sreedhar, and C. R. Patra, "Potential therapeutic and diagnostic applications of one-step in situ biosynthesized gold nanoconjugates (2-in-1 system) in cancer treatment," RSC Advances, vol. 3, no. 7, pp. 2318–2329, 2013.
11) Q. Li, S. Mahendra, D. Y. Lyon et al., "Antimicrobial nanomaterials for water disinfection and microbial control: potential applications and implications," Water Research, vol. 42, no. 18, pp. 4591–4602, 2008.
12) S. Dehghanizade, J. Arasteh, and A. Mirzaie, "Green synthesis of silver nanoparticles usingAnthemis atropatanaextract: characterization andin vitrobiological activities," Artificial Cells, Nanomedicine, and Biotechnology, vol. 46, no. 1, pp. 160– 168, 2018.
13) H. E. A. Mohamed, S. Afridi, A. T. Khalil et al., "Biosynthesis of silver nanoparticles from Hyphaene thebaica fruits and theirin vitropharmacognostic potential," Materials Research Express, vol. 6, no. 10, p. 1050c9, 2019.

14) S. Iravani, H. Korbekandi, S. Mirmohammadi, and B. Zolfaghari, "Synthesis of silver nanoparticles: chemical, physical and biological methods," Research in pharmaceutical sciences, vol. 9, p. 385, 2014.
15) A. Diallo, B. D. Ngom, E. Park, and M. Maaza, "Green synthesis of ZnO nanoparticles by Aspalathus linearis: structural & optical properties," Journal of Alloys and Compounds, vol. 646, pp. 425–430, 2015.
16) A. K. Zak, W. H. B. A. M. Razali, and M. Darroudi, "Synthesis and characterization of a narrow size distribution of zinc oxide nanoparticles," International Journal of Nanomedicine, vol. 6, p. 1399, 2011.
17) M. K. Swamy, K. M. Sudipta, K. Jayanta, and S. Balasubramanya, "The green synthesis, characterization, and evaluation of the biological activities of silver nanoparticles synthesized from Leptadenia reticulata leaf extract," Applied Nanoscience, vol. 5, no. 1, pp. 73–81, 2015.
18) J. Y. Song and B. S. Kim, "Rapid biological synthesis of silver nanoparticles using plant leaf extracts," Bioprocess and Biosystems Engineering, vol. 32, no. 1, pp. 79–84, 2009.
19) F. Erci, R. Cakir-Koc, and I. Isildak, "Green synthesis of silver nanoparticles using Thymbra spicata L. var. spicata (zahter) aqueous leaf extract and evaluation of their morphologydependent antibacterial and cytotoxic activity," Artificial cells, nanomedicine, and biotechnology, vol. 46, no. sup1, pp. 150– 158, 2018.
20) H. Singh, J. Du, and T.-H. Yi,"Green and rapid synthesis of silver nanoparticles usingBorago officinalisleaf extract: anticancer and antibacterial activities," Artificial Cells, Nanomedicine, and Biotechnology, vol. 45, no. 7, pp. 1310– 1316, 2016.
21) Albach, Dirk C., Zoya M. Tsymbalyuk, and Sergei L. Mosyakin. "Pollen morphology of Ellisiophyllum and Sibthorpia (Plantaginaceae, tribe Sibthorpieae) and phylogenetics of the tribe." *Plant Systematics and Evolution* 307.6 (2021): 66.
22) M. Lam, A. R. Carmichael, and H. R. Griffiths, "An aqueous extract of Fagonia cretica induces DNA damage, cell cycle arrest and apoptosis in breast cancer cells via FOXO3a and p 53 expression," Plo S one, vol. 7, no. 6, article e40152, 2012.
23) K. Venugopal, H. A. Rather, K. Rajagopal et al., "Synthesis of silver nanoparticles (Ag NPs) for anticancer activities (MCF 7 breast and A549 lung cell lines) of the crude extract of Syzygium aromaticum," Journal of Photochemistry and Photobiology B: Biology, vol. 167, pp. 282–289, 2017.
24) I. Ullah, E. Ş. Abamor, M. Bağirova, Z. K. Shinwari, and A. M. Allahverdiyev, "Biomimetic production, characterisation, in vitro cytotoxic and anticancer assessment of aqueous extract-mediated AgNPs of Teucrium stocksianum Boiss," IET Nanobiotechnology, vol. 12, no. 3, pp. 270–276, 2018.

25) P. Yugandhar and N. Savithramma, "Biosynthesis, characterization and antimicrobial studies of green synthesized silver nanoparticles from fruit extract of Syzygium alternifolium (Wt.) Walp. An endemic, endangered medicinal tree taxon," Applied Nanoscience, vol. 6, no. 2, pp. 223–233, 2016.
26) Y. Rout, S. Behera, A. K. Ojha, and P. Nayak, "Green synthesis of silver nanoparticles using Ocimum sanctum (Tulashi) and study of their antibacterial and antifungal activities," Journal of Microbiology and Antimicrobials, vol. 4, no. 6, pp. 103– 109, 2012.
27) A. Petica, S. Gavriliu, M. Lungu, N. Buruntea, and C. Panzaru, "Colloidal silver solutions with antimicrobial properties," Materials Science and Engineering: B, vol. 152, no. 1-3, pp. 22–27, 2008. [
28) H. Padalia, P. Moteriya, and S. Chanda,"Green synthesis of silver nanoparticles from marigold flower and its synergistic antimicrobial potential," Arabian Journal of Chemistry, vol. 8, no. 5, pp. 732–741, 2015.
29) R. Janthima, A. Khamhaengpol, and S. Siri, "Egg extract of apple snail for eco-friendly synthesis of silver nanoparticles and their antibacterial activity," Artificial Cells, Nanomedicine, and Biotechnology, vol. 46, no. 2, pp. 361–367, 2017.
30) K. Vasanth, K. Ilango, R. MohanKumar, A. Agrawal, and G. P. Dubey, "Anticancer activity of Moringa oleifera mediated silver nanoparticles on human cervical carcinoma cells by apoptosis induction," Colloids and Surfaces B: Biointerfaces, vol. 117, pp. 354–359, 2014.
31) D. Raghunandan, B. Ravishankar, G. Sharanbasava et al., "Anti-cancer studies of noble metal nanoparticles synthesized using different plant extracts," Cancer Nanotechnology, vol. 2, no. 1-6, pp. 57–65, 2011.
32) A. M. Shawkey, M. A. Rabeh, A. K. Abdulall, and A. O. Abdellatif, "Green nanotechnology: anticancer activity of sinver Nanoparticles using Citrullus colocynthis aqueous extracts," Advances in Life Science and Technology, vol. 13, pp. 60–70, 2013.
33) H. Saad, M. I. Soliman, A. M. Azzam, and B. Mostafa, "Antiparasitic activity of silver and copper oxide nanoparticles against Entamoeba histolytica and Cryptosporidium parvum cysts," Journal of the Egyptian Society of Parasitology, vol. 45, no. 3, pp. 593–602, 2015.
34) A. M. Allahverdiyev, E. S. Abamor, M. Bagirova et al., "Antileishmanial effect of silver nanoparticles and their enhanced antiparasitic activity under ultraviolet light," International Journal of Nanomedicine, vol. 6, pp. 2705–2714, 2011.
35) S. Yadegari-Dehkordi, H. R. Sadeghi, N. Attaran-Kakhki, M. Shokouhi, and A. Sazgarnia, "Silver nanoparticles increase cytotoxicity induced by intermediate frequency low voltages," Electromagnetic Biology and Medicine, vol. 34, pp. 317–321, 2014.

36) T. Y. Suman, S. R. R. Rajasree, A. Kanchana, and S. B. Elizabeth, "Biosynthesis, characterization and cytotoxic effect of plant mediated silver nanoparticles using Morinda citrifolia root extract," Colloids and Surfaces B: Biointerfaces, vol. 106, pp. 74–78, 2013.

37) B. Kulandaivelu and K. M. Gothandam, "Cytotoxic effect on cancerous cell lines by biologically synthesized silver nanoparticles," Brazilian Archives of Biology and Technology, vol. 59, 2016.

38) E.-J. Park, J. Yi, Y. Kim, K. Choi, and K. Park, "Silver nanoparticles induce cytotoxicity by a Trojan-horse type mechanism," Toxicology In Vitro, vol. 24, no. 3, pp. 872–878, 2010.

39) M. I. Sriram, S. B. M. Kanth, K. Kalishwaralal, and S. Gurunathan, "Antitumor activity of silver nanoparticles in Dalton's lymphoma ascites tumor model," International Journal of Nanomedicine, vol. 5, p. 753, 2010.

40) E. Z. Gomaa,"Antimicrobial, antioxidant and antitumor activities of silver nanoparticles synthesized by Allium cepa extract: a green approach," Journal of Genetic Engineering and Biotechnology, vol. 15, no. 1, pp. 49–57, 2017.

41) P. Sanpui, A. Chattopadhyay, and S. S. Ghosh, "Induction of apoptosis in cancer cells at low silver nanoparticle concentrations using chitosan nanocarrier," ACS Applied Materials & Interfaces, vol. 3, no. 2, pp. 218–228, 2011.

42) H. Ozer, J. O. Armitage, C. L. Bennett et al., "2000 update of recommendations for the use of hematopoietic colonystimulating factors: evidence-based, clinical practice guidelines," Journal of Clinical Oncology, vol. 18, no. 20, pp. 3558– 3585, 2000.

43) Otunola, Gloria Aderonke, and Anthony Jide Afolayan. "In vitro antibacterial, antioxidant and toxicity profile of silver nanoparticles green-synthesized and characterized from aqueous extract of a spice blend formulation." *Biotechnology & Biotechnological Equipment* 32.3 (2018): 724-733.

44) Singh, Hina, et al. "Ecofriendly synthesis of silver and gold nanoparticles by Euphrasia officinalis leaf extract and its biomedical applications." *Artificial cells, nanomedicine, and biotechnology* 46.6 (2018): 1163-1170.

45) Kornyakov, Ilya V., et al. "Synthesis, characterization and morphotropic transitions in a family of M [(UO2)(CH3COO) 3](H2O) n (M= Na, K, Rb, Cs; n= 0–1.0) compounds." *Zeitschrift für Kristallographie-Crystalline Materials* 235.3 (2020): 95-103.

46) Pratiwi, Risha, and Yati Nurlaeni. "Screening of plant collection of Cibodas Botanic Gardens, Indonesia with anticancer properties." *Biodiversitas Journal of Biological Diversity* 21.11 (2020).

47) J. C. Stockert, A. Blázquez-Castro, M. Cañete, R. W. Horobin, and Á. Villanueva, "MTT assay for cell viability: intracellular localization of the formazan product is in lipid droplets," Acta Histochemica, vol. 114, no. 8, pp. 785–796, 2012.

48) S. Kasibhatla, G. P. Amarante-Mendes, D. Finucane, T. Brunner, E. Bossy-Wetzel, and D. R. Green, "Acridine orange/ethidium bromide (AO/EB) staining to detect apoptosis," Cold Spring Harbor Protocols, vol. 2006, no. 21, 2006.

49) S. Machana, N. Weerapreeyakul, S. Barusrux, K. Thumanu, and W. Tanthanuch, "Synergistic anticancer effect of the extracts from Polyalthia evecta caused apoptosis in human hepatoma (HepG2) cells," Asian Pacific Journal of Tropical Biomedicine, vol. 2, no. 8, pp. 589–596, 2012.

50) A. M. Rieger, K. L. Nelson, J. D. Konowalchuk, and D. R. Barreda, "Modified annexin V/propidium iodide apoptosis assay for accurate assessment of cell death," Journal of visualized experiments, vol. 50, article e2597, 2011.

51) Derrien, Thomas, et al. "The GENCODE v7 catalog of human long noncoding RNAs: analysis of their gene structure, evolution, and expression." *Genome research* 22.9 (2012): 1775-1789.

52) X. Wang and M. G. Roper,"Measurement of DCF fluorescence as a measure of reactive oxygen species in murine islets of Langerhans," Analytical Methods, vol. 6, no. 9, pp. 3019–3024, 2014.

53) Mourão, Paulo AS, and Mariana S. Pereira. "Searching for alternatives to heparin: sulfated fucans from marine invertebrates." *Trends in Cardiovascular Medicine* 9.8 (1999): 225-232.

54) M. Ovais, A. T. Khalil, A. Raza et al., "Green synthesis of silver nanoparticles via plant extracts: beginning a new era in cancer theranostics," Nanomedicine, vol. 11, no. 23, pp. 3157–3177, 2016.

55) M. Darroudi, Z. Sabouri, R. Kazemi Oskuee, A. Khorsand Zak, H. Kargar, and M. H. N. Abd Hamid, "Green chemistry approach for the synthesis of ZnO nanopowders and their cytotoxic effects," Ceramics International, vol. 40, no. 3, pp. 4827–4831, 2014.

56) D. Puri and A. Bhandari, "Fagonia: a potential medicinal desert plant," Journal of Nepal Pharmaceutical Association, vol. 27, no. 1, pp. 28–33, 2015.

57) Ashraf, Jalaluddin M., et al. "Green synthesis of silver nanoparticles and characterization of their inhibitory effects on AGEs formation using biophysical techniques." *Scientific reports* 6.1 (2016): 1-10.

58) Alamier, W. M., DY Oteef, M., Bakry, A. M., Hasan, N., Ismail, K. S., & Awad, F. S. (2023). Green Synthesis of Silver Nanoparticles Using Acacia ehrenbergiana Plant Cortex Extract for Efficient Removal of Rhodamine B Cationic Dye from Wastewater and the Evaluation of Antimicrobial Activity. *ACS omega*.

59) S. P. Dubey, M. Lahtinen, and M. Sillanpää, "Tansy fruit mediated greener synthesis of silver and gold nanoparticles," Process Biochemistry, vol. 45, no. 7, pp. 1065–1071, 2010.

60) I. Ullah, Z. K. Shinwari, and K. ATJPJB, "Investigation of the cytotoxic and antileishmanial effects of Fagonia indica L. extract and extract mediated silver nanoparticles (AgNPs)," Pakistan Journal of Botany, vol. 49, pp. 1561–1568, 2017.

61) P. Prakash, P. Gnanaprakasam, R. Emmanuel, S. Arokiyaraj, and M. Saravanan, "Green synthesis of silver nanoparticles from leaf extract of Mimusops elengi, Linn. for enhanced antibacterial activity against multi drug resistant clinical isolates," Colloids and Surfaces B: Biointerfaces, vol. 108, pp. 255–259, 2013.

62) B. Ajitha, Y. Ashok Kumar Reddy, and P. S. Reddy, "Biogenic nano-scale silver particles by Tephrosia purpurea leaf extract and their inborn antimicrobial activity," Spectrochimica Acta Part A: Molecular and Biomolecular Spectroscopy, vol. 121, pp. 164–172, 2014.

63) V. S. Kotakadi, Y. S. Rao, S. A. Gaddam, T. N. V. K. V. Prasad, A. V. Reddy, and D. V. R. S. Gopal, "Simple and rapid biosynthesis of stable silver nanoparticles using dried leaves of Catharanthus roseus. Linn. G. Donn and its anti microbial activity," Colloids and Surfaces B: Biointerfaces, vol. 105, pp. 194–198, 2013.

64) K. Anandalakshmi, J. Venugobal, and V. Ramasamy, "Characterization of silver nanoparticles by green synthesis method using Pedalium murex leaf extract and their antibacterial activity," Applied Nanoscience, vol. 6, no. 3, pp. 399–408, 2016

65) R. R. Remya, S. R. R. Rajasree, L. Aranganathan, and T. Y. Suman, "An investigation on cytotoxic effect of bioactive AgNPs synthesized using Cassia fistula flower extract on breast cancer cell MCF-7," Biotechnology Reports, vol. 8, pp. 110–115, 2015.

66) C. Krishnaraj, R. Ramachandran, K. Mohan, and P. T. Kalaichelvan, "Optimization for rapid synthesis of silver nanoparticles and its effect on phytopathogenic fungi," Spectrochimica Acta Part A: Molecular and Biomolecular Spectroscopy, vol. 93, pp. 95–99, 2012.

67) A. Rautela, J. Rani, M.D. Das Green synthesis of silver nanoparticles from Tectona grandis seeds extract: characterization and mechanism of antimicrobial action on different microorganisms.

68) P. Devaraj, P. Kumari, C. Aarti, A. Renganathan Synthesis and characterization of silver nanoparticles using cannonball leaves and their cytotoxic activity against MCF-7 cell line J. Nanotechnol. (2013), Article 598328, 10.1155/2013/598328

69) P. Devaraj, P. Kumari, C. Aarti, A. Renganathan Synthesis and characterization of silver nanoparticles using cannonball leaves and their cytotoxic activity against MCF-7 cell line J. anotechnol. (2013),article 598328, 10.1155/2013/598328

70) E.K. Kambale, C.I. Nkanga, B.-P.I. Mutonkole, A.M. Bapolisi, D.O. Tassa, J.-M.I. Liesse, R.W. Krause, P.B. Memvanga Green synthesis of antimicrobial silver nanoparticles using aqueous leaf extracts from three Congolese plant species *Brillantaisia patula, Crossopteryx febrifuga* and *Senna siamea*) Heliyon, 6 (8) (2020), Article e04493, 10.1016/j.heliyon.2020.e04493

71) R. Vivek, R. Thangam, K. Muthuchelian, P. Gunasekaran, K. Kaveri, and S. Kannan, "Green biosynthesis of silver nanoparticles from Annona squamosa leaf extract and its in vitro cytotoxic effect on MCF-7 cells," Process Biochemistry, vol. 47, no. 12, pp. 2405–2410, 2012.

72) S. A. Sadat Shandiz, M. Shafiee Ardestani, D. Shahbazzadeh et al., "Novel imatinib-loaded silver nanoparticles for enhanced apoptosis of human breast cancer MCF-7 cells," Artificial cells, nanomedicine, and biotechnology, vol. 45, no. 6, pp. 1082–1091, 2017.

73) L. Inbathamizh, T. M. Ponnu, and E. J. Mary, "In vitro evaluation of antioxidant and anticancer potential of Morinda pubescens synthesized silver nanoparticles," Journal of Pharmacy Research, vol. 6, no. 1, pp. 32–38, 2013.

74) K. Venugopal, H. Ahmad, E. Manikandan et al., "The impact of anticancer activity upon Beta vulgaris extract mediated biosynthesized silver nanoparticles (Ag-NPs) against human breast (MCF-7), lung (A549) and pharynx (Hep-2) cancer cell lines," Journal of Photochemistry and Photobiology B: Biology, vol. 173, pp. 99–107, 2017.

75) M. Ramar, B. Manikandan, P. N. Marimuthu et al., "Synthesis of silver nanoparticles using Solanum trilobatum fruits extract and its antibacterial, cytotoxic activity against human breast cancer cell line MCF 7," Spectrochimica Acta Part A: Molecular and Biomolecular Spectroscopy, vol. 140, pp. 223–228, 2015.

76) H. Ciftci, M. TÜRK, U. TAMER, S. Karahan, and Y. Menemen, "Silver nanoparticles: cytotoxic, apoptotic, and necrotic effects on MCF-7 cells," Turkish Journal of Biology, vol. 37, pp. 573–581, 2013.

77) S. S. Bhattacharyya, S. K. Mandal, R. Biswas et al., "In vitro studies demonstrate anticancer activity of an alkaloid of the plant Gelsemium sempervirens," Experimental Biology and Medicine, vol. 233, no. 12, pp. 1591–1601, 2008.

78) V. Kathiravan, S. Ravi, and S. Ashokkumar,"Synthesis of silver nanoparticles from Melia dubia leaf extract and their in vitro anticancer activity," Spectrochimica Acta Part A: Molecular

79) Dwivedi S, Siddiqui M A, Farshori N N, Ahamed M, MusarratJ, and Al-Khedhairy A A (2014) Synthesis, characterization and toxicological evaluation of iron oxide nanoparticles in human lung alveolar epithelial cells, Colloids and Surfaces B: Bio interfaces, 122: 209–215

80) NicolettiI., G. Migliorati, M. C. Pagliacci, F. Grignani, and C. Riccardi, 1991. A rapid and simple method for measuring thymocyte apoptosis by propidium iodide staining and flow cytometry, Journal of Immunological Methods, 139(2): 271–279.

81) Ravi. S., K. K. Chiruvella, K. Rajesh, V. Prabhu, and S. C. Raghavan, (2010). 5-isopropylidene3-ethylrhodanine induce growth inhibition followed by apoptosis in leukemia cells, European Journal of Medicinal Chemistry, vol. 45, no. 7, pp. 2748–2752.

82) J. Liang, F. Zeng, M. Zhang et al., "Green synthesis of hyaluronic acid-based silver nanoparticles and their enhanced delivery to CD44+ cancer cells," RSC Advances, vol. 5, no. 54, pp. 43733–43740, 2015.

83) D. R. McIlwain, T. Berger, and T. W. Mak, "Caspase functions in cell death and disease," Cold Spring Harbor Perspectives in Biology, vol. 5, p. a008656, 2013.

84) Y. Shi, "Mechanisms of caspase activation and inhibition during apoptosis," Molecular Cell, vol. 9, no. 3, pp. 459–470, 2002.

85) K. M. Boatright, M. Renatus, F. L. Scott et al., "A unified model for apical caspase activation," Molecular Cell, vol. 11, no. 2, pp. 529–541, 2003.

86) S. J. Riedl and Y. Shi, "Molecular mechanisms of caspase regulation during apoptosis," Nature Reviews Molecular Cell Biology, vol. 5, no. 11, pp. 897–907, 2004.

87) G. M. Cohen, "Caspases: the executioners of apoptosis," Biochemical Journal, vol. 326, no. 1, pp. 1–16, 1997.

88) M. Kikuchi, S. Kuroki, M. Kayama, S. Sakaguchi, K.-K. Lee, and S. Yonehara, "Protease activity of procaspase-8 is essential for cell survival by inhibiting both apoptotic and nonapoptotic cell death dependent on receptor-interacting protein kinase 1 (RIP1) and RIP3," Journal of Biological Chemistry, vol. 287, no. 49, pp. 41165–41173, 2012.

89) B. C. G. Selvi, J. Madhavan, and A. Santhanam, "Cytotoxic effect of silver nanoparticles synthesized from Padina tetrastromatica on breast cancer cell line," Advances in Natural Oxidative Medicine and Cellular Longevity 13 Sciences: Nanoscience and Nanotechnology, vol. 7, p. 035015, 2016.

90) H. Nakajima, J. Magae, M. Tsuruga et al., "Induction of mitochondria-dependent apoptosis through the inhibition of mevalonate pathway in human breast cancer cells by YM529, a new third generation bisphosphonate," Cancer Letters, vol. 253, no. 1, pp. 89–96, 2007.

91) J. Ma, di Zhao, H. Lu, W. Huang, and D. Yu, "Apoptosis signal-regulating kinase 1 (ASK1) activation is involved in silver nanoparticles induced apoptosis of A549 lung cancer cell line," Journal of Biomedical Nanotechnology, vol. 13, no. 3, pp. 349–354, 2017.

92) A. H. Wyllie, "Glucocorticoid-induced thymocyte apoptosis is associated with endogenous endonuclease activation," Nature, vol. 284, no. 5756, pp. 555-556, 1980.

93) S. Arora, J. Jain, J. M. Rajwade, and K. M. Paknikar, "Cellular responses induced by silver nanoparticles: in vitro studies," Toxicology Letters, vol. 179, no. 2, pp. 93–100, 2008.

94) A. Nel, T. Xia, L. Mädler, and N. Li, "Toxic potential of materials at the nanolevel," science, vol. 311, no. 5761, pp. 622–627, 2006.

95) H. Li, J. Chen, C. Xiong, H. Wei, C. Yin, and J. Ruan, "Apoptosis induction by the total flavonoids from Arachniodes exilis in HepG2 cells through reactive oxygen species-mediated mitochondrial dysfunction involving MAPK activation," Evidence-based Complementary and Alternative Medicine, vol. 2014, 11 pages, 2014.

96) N. Lampiasi, A. Azzolina, N. D'Alessandro et al., "Antitumor effects of dehydroxymethylepoxyquinomicin, a novel nuclear factor-κB inhibitor, in human liver cancer cells are mediated through a reactive oxygen species-dependent mechanism," Molecular Pharmacology, vol. 76, no. 2, pp. 290–300, 2009.

97) Y.-H. Hsin, C.-F. Chen, S. Huang, T.-S. Shih, P.-S. Lai, and P. J. Chueh, "The apoptotic effect of nanosilver is mediated by a ROS- and JNK-dependent mechanism involving the mitochondrial pathway in NIH3T3 cells," Toxicology Letters, vol. 179, no. 3, pp. 130–139, 2008.

98) H. J. Forman and M. Torres, "Reactive oxygen species and cell signaling," American Journal of Respiratory and Critical Care Medicine, vol. 166, supplement_1, pp. S4–S8, 2002.